

# ITERATIVE FITTING AFTER ELASTIC REGISTRATION: AN EFFICIENT STRATEGY FOR ACCURATE ESTIMATION OF PARAMETRIC DEFORMATIONS

Xinxin Zhang, Christopher Gilliam and Thierry Blu

Department of Electronic Engineering, The Chinese University of Hong Kong, Hong Kong

## ABSTRACT

We propose an efficient method for image registration based on iteratively fitting a parametric model to the output of an elastic registration. It combines the flexibility of elastic registration - able to estimate complex deformations - with the robustness of parametric registration - able to estimate very large displacement. Our approach is made feasible by using the recent Local All-Pass (LAP) algorithm; a fast and accurate filter-based method for estimating the local deformation between two images. Moreover, at each iteration we fit a linear parametric model to the local deformation which is equivalent to solving a linear system of equations (very fast and efficient). We use a quadratic polynomial model however the framework can easily be extended to more complicated models. The significant advantage of the proposed method is its robustness to model mis-match (e.g. noise and blurring). Experimental results on synthetic images and real images demonstrate that the proposed algorithm is highly accurate and outperforms a selection of image registration approaches.

**Index Terms**— Image registration, Iterative fitting, Elastic registration, Parametric registration, Local All-Pass filters

## 1. INTRODUCTION

Image registration plays an important role in clinical applications [1, 2], remote sensing [3], and many other fields of modern science. Aligning two or more images of the same scene taken from different view points or at different times, is known as monomodal image registration. In contrast, aligning images of the same scene taken by different sensors is known as multimodal registration. In this paper, we focus on monomodal image registration that involves two images. One of them is referred to as the target image and the other is the source image, and they are denoted by  $I_1$  and  $I_2$ , respectively. Under the assumption of brightness consistency [4], these images are related by a displacement field  $u(x, y) = (u_1(x, y), u_2(x, y))$  as follows:

$$I_1(x, y) = I_2(x + u_1(x, y), y + u_2(x, y)), \quad (1)$$

This work was supported in part by a grant #CUHK14200114 of the Hong Kong Research Grants Council.

where  $(x, y)$  is the pixel coordinate. Thus, the key task of image registration is to estimate the displacement field  $u$  such that  $I_2$  is aligned to  $I_1$ .

In recent years, a variety of methods have been proposed for image registration. These methods can be roughly split into three groups. The first group [5, 6, 7] use a global parametric model to describe the displacement field, so the registration problem reduces to calculating the parameters of the model (i.e. fast to compute). For example a linear polynomial comprising 6 parameters can model transformations such as translation, rotation and scaling [5]. However, as the complexity of the displacement field increases more model parameters are required and their estimation becomes prone to local minima. In contrast, the second group of methods [8, 9, 10, 11, 12, 13, 14] perform elastic registration and estimate a displacement vector per pixel. Such methods can represent local, complex, distortions but are prone to model mis-match [15] and require long run-times. The final group are feature-based methods [16, 17, 18, 19] in which the displacement is estimated by establishing the correspondence between the extracted features or landmarks from the two images. The performance of these methods are closely associated with the feature types and the accuracy of the feature detection. Although many of the above approaches perform well in some particular scenarios, none are consistently robust in all cases [1, 2].

In this paper, we present a novel method for parametric image registration based on iteratively fitting the output of an elastic registration. More precisely, we first use the recently developed Local All-Pass (LAP) algorithm [20, 21] to obtain an estimate of the local deformation field and then fit a parametric model to this estimate. This process is then iterated until we obtain an accurate registration. The advantages of this method are three-fold: firstly, by combining local estimation with a global model, the approach can very accurately estimate deformations with both very large and very small displacements. Secondly, as we are fitting very few parameters to a dense deformation field, it is very robust to violations of the brightness consistency. Finally, it is flexible, we can easily change the type and complexity of the parametric model in the fitting process. We demonstrate these advantages using both synthetic and real images. In particular, we show our algorithm is more accurate and robust under noise, image

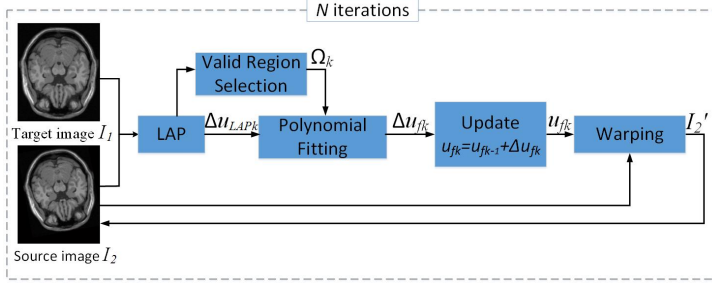


**Fig. 1.** Diagram illustrating the flow chart of the proposed iterative fitting method, in which  $\Delta u_{LAPk}$ ,  $\Delta u_{fk}$  and  $\Omega_k$  are the displacement increment estimated by the LAP algorithm and obtained by polynomial fitting and valid region in the  $k$ th iteration respectively.  $u_{fk}$  is the displacement between the original source image and the target image.

blur and information loss than a selection of standard image registration algorithms.

Importantly, in contrast to many elastic registration methods, the LAP algorithm is very fast - on the order of seconds to compute a dense deformation field [20, 21] - thus allowing our iterative framework to be a practical approach to the registration problem. This is supported by our experimental results.

## 2. REGISTRATION BY ITERATIVE FITTING

In this section we present our iterative image registration method. At each iteration, our method contains three key steps: estimating the local deformation using the LAP algorithm, parametric fitting using a polynomial function and selection of a valid region in which to perform the fitting. The technical details of these key steps are described in the rest of this article and their connection to each other is illustrated in Fig. 1.

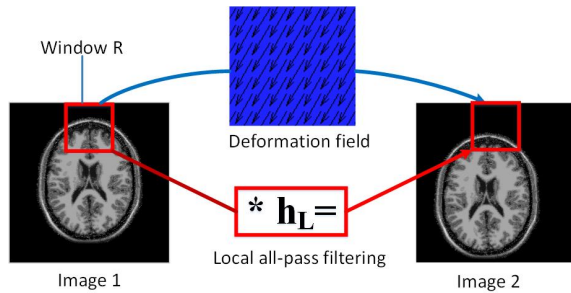


**Fig. 2.** Diagram illustrating the equivalence of constant displacement field and filtering with an all-pass filter within a window. The local deformation field in the window  $R$  is extracted from the local all-pass filter.  $*$  denotes the convolution operator and  $h_L$  is the local all-pass filter of the window.

### 2.1. Elastic Registration using Local All-Pass Filters

Recently, Gilliam and Blu [20, 21] proposed a fast and accurate filter-based algorithm to estimate the deformation between two images, which is termed Local All-Pass (LAP) algorithm. The main idea of this method is that the two images can be related, on a local level, using an all-pass filter and the displacement extracted from the filter, an example is shown in Fig. 2. This process is then repeated for every pixel in the image to obtain a dense deformation estimate.

Compared with the state-of-the-art elastic registration methods, the LAP algorithm has three significant advantages. First, it is a highly accurate algorithm when estimating a deformation in which the brightness constraint is exactly satisfied. Second, it is robust to violations of the brightness consistency caused by noise corruption or illumination change. Third, it does not require complex computation thus is very fast and efficient.

However, although the LAP algorithm is accurate in most cases, there are situations where it does not perform perfectly. For example, the LAP relies upon the assumption that the deformation is locally constant thus it struggles when deformation is very large and highly non-constant (e.g. rotations). Another situation is when the brightness consistency is violated by degradation such as image blur or loss of information. It is these defects that we wish to remedy with our fitting approach.

### 2.2. Parametric fitting using a polynomial function

For this paper, we restrict the scope of our parametric fitting to a polynomial model. Specifically, the fitting model we use is a second order polynomial function:

$$u_f(z) = c_1 + c_2 z + c_3 \bar{z} + c_4 z \bar{z} + c_5 z^2 + c_6 \bar{z}^2, \quad (2)$$

where  $z = x + iy$ ,  $\bar{z} = x - iy$  is the complex conjugate of  $z$ ,  $x$  and  $y$  are the vertical coordinate and horizontal coordinate of a pixel, respectively.  $c_1, c_2, c_3, c_4, c_5$  and  $c_6$  are the unknown coefficients, and they are all complex numbers. As  $u$  is a vector field, it can easily be represented using a complex number. Thus we use the following notation  $u(z) = u_1(z) + i * u_2(z)$  to represent the vector field  $u$ .

In the proposed method, estimating the displacement on a global level is equivalent to calculating the six coefficients in (2). They are obtained from the minimization of the difference between  $\Delta u_{LAP}$  and  $\Delta u_f$ . Therefore, we minimize the following energy function:

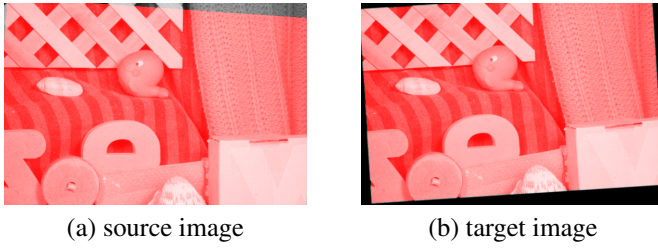
$$\min_c \sum_{z \in \Omega} |\Delta u_f(z) - \Delta u_{LAP}(z)|^2, \quad (3)$$

where  $c = [c_1, c_2, c_3, c_4, c_5, c_6]^T$  and  $\Omega$  is the valid region which will be described in detail in Section 2.3. The solution to (3) is equivalent to solving a linear system of equations which is fast and efficient.

**Table 1.** Error comparison for the iterative fitting method and the state-of-the-art image registration methods.

		Noiseless Image			Noisy Image (15dB)			Gaussian Blurry Image			Missing Information		
		$E_{Med}$	$E_{Mean}$	Time	$E_{Med}$	$E_{Mean}$	Time	$E_{Med}$	$E_{Mean}$	Time	$E_{Med}$	$E_{Mean}$	Time
Parametric algorithms	Ours	<b>0</b>	<b>0</b>	18.45	<b>0.238</b>	<b>0.430</b>	19.08	<b>0.505</b>	<b>0.590</b>	32.22	<b>0</b>	<b>0</b>	38.58
	AECC [22]	0.851	1.155	9.10	0.908	1.229	9.522	1.001	1.289	8.10	0.907	1.206	9.32
Elastic algorithms	LAP [20]	0.006	1.189	<b>4.60</b>	1.799	4.076	<b>4.52</b>	3.118	3.415	<b>5.94</b>	0.011	2.131	<b>7.94</b>
	Demons [23]	5.114	32.874	37.15	7.601	10.241	22.13	6.066	7.497	31.75	5.700	10.575	20.81
	MIRT [24]	3.232	9.931	75.00	7.976	12.065	52.51	7.420	11.467	65.67	7.764	12.661	80.00
	bUnwarpJ [8]	1.3402	1.4107	14.64	1.6763	1.8072	25.07	3.346	4.512	23.80	1.924	7.220	325.38

(1) Bold values indicate the best results. (2) The size of images is 388 by 584 pixels. (3) PSNR between the noisy image and original noiseless image is 15dB. (4) The largest displacement is 61 pixels.

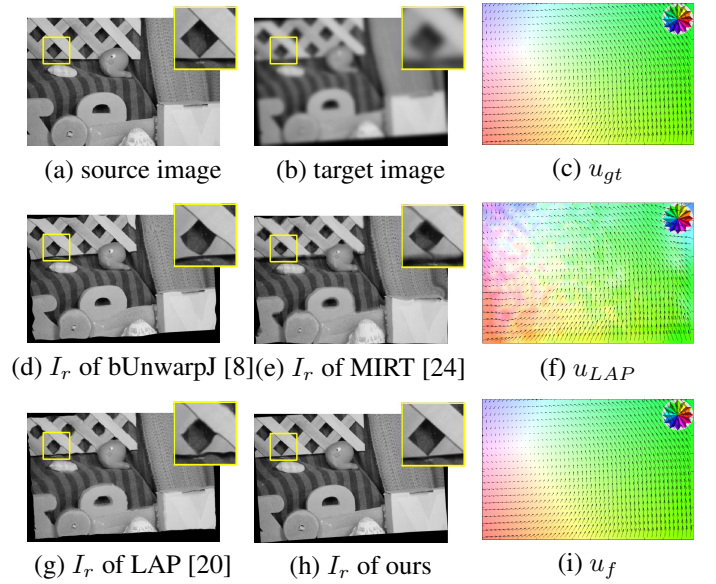
**Fig. 3.** Diagram illustrating the common region (marked in red) of source image and target image.

After obtaining the coefficients, the parametric displacement field is used to warp the source image closer to the target image. Since the estimated displacement is non-integer, it is essential to build a continuous model of image for image warping. We adopt the shifted linear interpolation [25] to obtain a high quality warped image.

### 2.3. Valid Region Selection - a robust region for fitting

Ideally we would use all available vectors of the deformation field to perform the fitting. In practice, however, some regions of the scene may only be visible in one image. Consequently the deformation estimate in these regions may be unreliable as the LAP algorithm works on a local level. Thus we need to identify a common region that exists in both images and use this region for the fitting. An example of the common region between the images to be registered is shown in Fig. 3. In a similar manner, we also want to exclude erroneous deformation estimates caused by brightness change, occlusion, missing information or noise. Therefore we want to refine the common region to a region where we have confidence in the deformation estimate - we call this the valid region. The valid region is obtained and updated every iteration as follows.

In the first iteration, we use the LAP algorithm to estimate the displacement  $\Delta u_{LAP}$  between the source image and target image. The 1st valid region,  $\Omega_1$ , is the set of pixels that

**Fig. 4.** Example of image registration on synthetic images. (c) is the ground-truth displacement field  $u_{gt}$ . The zoom-in regions in the yellow rectangle are shown in the top-right corner in the image.

remain within the bounds of the target image when warping the source image with  $\Delta u_{LAP}$ . In the following iterations, we obtain a new common region using  $\Delta u_{f(k-1)}$  and sort the amplitude of  $\Delta u_{LAP}$  in this region from small to large. The top 50 percent of the sorted values of  $\Delta u_{LAP}$  are then set to be the valid region  $\Omega_k$ , where  $k$  is the number of iteration.

## 3. EXPERIMENTAL RESULTS

In this section, extensive experiments are performed on both synthetic images and real images with the proposed method. We compare our method with the LAP algorithm [20] and other four well-known registration methods: intensity-based

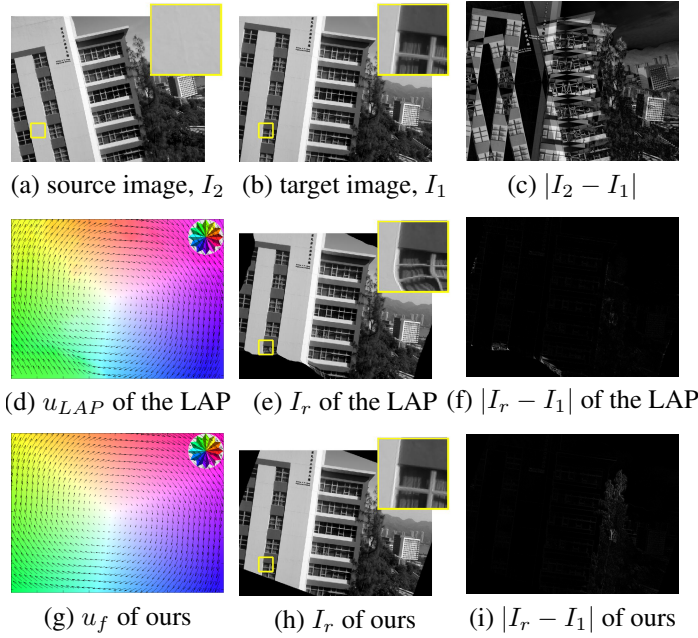


**Fig. 5.** Example of image registration on real images. (c) is the absolute difference between the source image and target image. (f) and (i) are the absolute difference between the registered image  $I_r$  and the target image of the LAP and the proposed method, respectively.

image registration using residual complexity minimisation from the Medical Image Registration Toolbox (MIRT) [24], parametric image alignment using enhanced correlation coefficient maximization (AECC) [10], the Demons algorithm based on the implementation in [23] and elastic registration using a cubic B-spline free form deformation model implemented in ImageJ (bUnwarpJ) [8]. The parameters of each method are set to its default values. In this paper, we set the iteration number to 5 for all the cases. All algorithms are run on an Intel Core i7-5557U 3.4 GHz with 4 GB RAM.

### 3.1. Synthetic images

To show the robustness of the proposed method, we generate synthetic deformation fields and four types of situations including noiseless images, noisy images, Gaussian blurry images and images of missing information. The evaluation results are shown in Table 1. Instead of evaluating the registered image quality directly, we evaluate the estimated displacement field by using the Median Absolute Error ( $E_{Med}$ ) and the Mean Absolute Error ( $E_{Mean}$ ). Note that the results are calculated in the common region and averaged over 5 different deformation fields. Also, the largest amplitude of displacement is 61 pixels. The table shows that the proposed method is highly accurate and outperforms the other methods significantly in terms of displacement accuracy. In terms of

computation time, the LAP algorithm is the fastest one. Note that the computation time of our method is not five times that of the LAP algorithm, because, as the iterations increase, the registered image becomes closer to the target image which reduces the computation time of the LAP. For the AECC algorithm, it is only effective for limited types of transformation with a low order. As the order becomes higher, however, it becomes unstable. An example of image registration on blurry images shown in Fig. 4 illustrates that the proposed method is robust to blur. Whereas parts (d), (e) and (g) illustrate the artifacts caused by the other registration algorithms. By comparing (f) and (i), we can see that the local inaccurate estimates from the LAP are remedied after iterative fitting.

### 3.2. Real images

To demonstrate the practicality of the proposed algorithm, we test our method on real photographs, captured from Huawei Honor camera phone. The registered results obtained by the LAP and the proposed method are shown in Fig. 5. For comparison, we show the absolute difference between the target image and registered image. The PSNR values are 31.97 dB and 30.94 dB, the SSIM values are 0.98 and 0.96 for the LAP and the proposed method, respectively. The computation time are 15.92 seconds and 96.97 seconds for the image of size 612 by 816 pixels, respectively. We note that the value of PSNR and SSIM are lower than that of the LAP algorithm, it is mainly because of the different depth of the tree and buildings. But we can run the LAP again with a very small window size to improve the result. The PSNR and SSIM values increase to 37.66 dB and 0.99, respectively. And this operation is very fast.

## 4. CONCLUSION

An efficient and accurate iterative fitting algorithm for image registration is proposed in this paper. The proposed method iteratively fits a parametric deformation field to the output of a fast elastic registration. More precisely, in each iteration, the LAP algorithm is applied to estimate the deformation on a local level. Then a polynomial function is used to fit this local displacement field and obtains a global, parametric, deformation. After that, the source image is warped to the target image. After several iterations, accurate displacement and high quality registered image are obtained. Extensive experiments showed that the proposed algorithm performs better than several methods in terms of image quality and computation time.

In the future work, the proposed method will be extended to solve multimodal registration, video stabilization and video deblurring problems. Furthermore, we will look at optimizing the method to make it more efficient. An obvious step is to combine the polynomial fitting with the LAP algorithm thus reducing the number of iterations required.



## 5. REFERENCES

- [1] A. Sotiras, C. Davatzikos, and N. Paragios, “Deformable medical image registration: A survey,” *IEEE Transactions on Medical Imaging*, vol. 32, pp. 1153–1190, 2013.
- [2] B. Zitova and J. Flusser, “Image registration methods: a survey,” *Image and Vision Computing*, vol. 21, pp. 977–1000, 2003.
- [3] S. Dawn, V. Saxena, and B. Sharma, “Remote sensing image registration techniques: A survey,” in *International Conference on Image and Signal Processing (IC-SIP)*, 2010, pp. 103–112.
- [4] S. Baker, D. Scharstein, and J. P. Lewis *et al.*, “A database and evaluation methodology for optical flow,” *International Journal of Computer Vision*, vol. 92, pp. 1–31, 2011.
- [5] R. Woods, S. Cherry, and J. Mazziotta, “Rapid automated algorithm for aligning and reslicing PET images,” *Journal of Computer Assisted Tomography*, vol. 16, pp. 620–633, 1992.
- [6] R. Woods, S. Grafton, and C. Holmes *et al.*, “Automated image registration: I. General methods and intrasubject, intramodality validation,” *Journal of Computer Assisted Tomography*, vol. 22, pp. 141–154, 1998.
- [7] F. Albu, “Low complexity image registration techniques based on integral projections,” in *International Conference on Systems, Signals and Image Processing (IWS-SIP)*, 2016, pp. 1–4.
- [8] I. Arganda-Carreras, C. O. S. Sorzano, and R. Marabini *et al.*, “Consistent and elastic registration of histological sections using vector-spline regularization,” in *International Workshop on Computer Vision Approaches to Medical Image Analysis (CVAMIA)*. Springer, 2006, pp. 85–95.
- [9] R. Bajcsy and S. Kovacic, “Multiresolution elastic matching,” *Computer Vision, Graphics and Image Processing*, vol. 46, pp. 1–21, 1989.
- [10] S. Periaswamy and H. Farid, “Elastic registration in the presence of intensity variations,” *IEEE Transactions on Medical Imaging*, vol. 22, pp. 865–874, 2003.
- [11] S. Klein, M. Staring, and K. Murphy *et al.*, “Elastix: a toolbox for intensity-based medical image registration,” *IEEE Transactions on Medical Imaging*, vol. 29, pp. 196–205, 2010.
- [12] S. Periaswamy and H. Farid, “Medical image registration with partial data,” *Medical Image Analysis*, vol. 10, pp. 452–464, 2006.
- [13] A. Goshtasby, “Image registration by local approximation methods,” *Image and Vision Computing*, vol. 6, pp. 255–261, 1988.
- [14] J. Kybic and M. Unser, “Fast parametric elastic image registration,” *IEEE Transactions on Image Processing*, vol. 12, pp. 1427–1442, 2003.
- [15] A. Bruhn, J. Weickert, and C. Schnorr, “Lucas/Kanade meets Horn/Schunck: Combining local and global optic flow methods,” *International Journal of Computer Vision*, vol. 61, pp. 211–231, 2005.
- [16] H. S. Alhichri, and M. Kamel, “Virtual circles: a new set of features for fast image registration,” *Pattern Recognition Letters*, vol. 24, pp. 1181–1190, 2003.
- [17] C. Davatzikos, J. L. Prince, and R. N. Bryan, “Image registration based on boundary mapping,” *IEEE Transactions on Medical Imaging*, vol. 15, pp. 112–115, 1996.
- [18] Q. Li, G. Wang, and J. Liu *et al.*, “Robust scale-invariant feature matching for remote sensing image registration,” *IEEE Geoscience and Remote Sensing Letters*, vol. 6, pp. 287–291, 2009.
- [19] J. Ma, W. Qiu, and J. Zhao *et al.*, “Robust  $L_2E$  estimation of transformation for non-rigid registration,” *IEEE Transactions on Signal Processing*, vol. 63, pp. 1115–1129, 2015.
- [20] C. Gilliam and T. Blu, “Local all-pass filters for optical flow estimation,” in *IEEE International Conference on Acoustics, Speech and Signal Processing (ICASSP)*, 2015, pp. 1533–1537.
- [21] C. Gilliam and T. Blu, “Local all-pass geometric deformations (submitted),” *IEEE Transactions on Image Processing*, 2017.
- [22] G. D. Evangelidis and E. Z. Psarakis, “Parametric image alignment using enhanced correlation coefficient maximization,” *IEEE Transactions on Pattern Analysis and Machine Intelligence*, vol. 30, pp. 1858–1865, 2008.
- [23] H. Lombaert, L. Grady, and X. Pennec *et al.*, “Diffeomorphic demons: Efficient non-parametric image registration,” *NeuroImage*, vol. 45, pp. S61–S72, 2009.
- [24] A. Myronenko and X. Song, “Intensity-based image registration by minimizing residual complexity,” *IEEE Transactions on Medical Imaging*, vol. 29, pp. 1882–1891, 2010.
- [25] T. Blu, P. Thévenaz, and M. Unser, “Linear interpolation revitalized,” *IEEE Transactions on Image Processing*, vol. 13, pp. 710–719, 2004.